Volume 64, Issue 1, 2020
Journal of Scientific Research
Institute of Science,
Banaras Hindu University, Varanasi, India.

Epitope Imprinting of Outer Membrane Protein of *Neisseria Meningitidis*

Neha Gupta[1], Juhi Srivastava[1], Lav Kumar Singh[1], Ambareesh K Singh[2], Kavita Shah[3], Rajniti Prasad[4], and Meenakshi Singh[1*]

[1]Department of Chemistry, MMV, Banaras Hindu University, Varanasi.
[2]Deaprtment of Chemistry, Institute of Science, Banaras Hindu University, Varanasi.
[3]Institute of Environment and Sustainable Development, Banaras Hindu University, Varanasi
[4]Department of Pediatrics, Institute of Medical Sciences, Banaras Hindu University, Varanasi.
meenakshi@bhu.ac.in, meenakshibhu70@gmail.com

Abstract: **Here, we report the development of an epitope-based electrochemical molecularly imprinted polymer (MIP)-sensor for the detection of Neisseria meningitidis by the electropolymerization of 3-thiophene acetic acid (3-TAA) on the gold surface of electrochemical quartz crystal microbalance EQCM. An epitope sequence GRHNSESYH is used here for designing a diagnostic tool via molecularly imprinting for N. meningitidis strain MC58. The imprinting of epitope sequences CGRHNSESYH, and its quantification on epitope imprinted polymer (EIP) was confirmed by electrochemical quartz crysal microbalance (EQCM), fluorescence spectroscopy, UV-visible spectroscopy and contact angle measurements as well as atomic force microscopy (AFM) imaging. The epitope-imprinted sensor shows an imprinting factor of 3.84 and limit of detection 9.87 ng ml-1 which indicates its feasibility for early diagnosis and disease monitoring without preclinical treatments.**

Index Terms: **Neisseria meningitides, Diagnostic tool, Epitope imprinted polymer, CGRHNSESYH, electrochemical quartz crystal microbalance.**

I. INTRODUCTION

Recently WHO has described Neisseria meningitidis bacteria as the potential carrier to cause large-scale epidemics. Timely diagnosis of this disease will be a boon for targeted population. It is currently being diagnosed by various diagnostic methods (Deivanayagam et al 1993, Sippel et al 1984, Surinder et al 2007, Tan et al 1987, Gray et al 1992, Dunbar et al 1998, Kilian et al 1979, Radstrom et al 1994, Neewcombe et al 1996, Kotilinen et al 1998, Carrol et al 2003, Baethegan et al 2003 Patel et al 2010), but these can diagnose the disease only at a later advanced stage when it has spread throughout the affected organs. Its early symptoms often lead to misdiagnosis leading to high rate of mortality. Hence, for long, a need for such a diagnostic technique is felt which can identify the culprit bacteria at an early stage and timely taken care of by clinical treatment at an opportune stage.

A viable approach for such an identification tool for disease causing bacteria can be via its protein, but selective identification of bacterial protein is an uphill task for biologists. Epitope imprinting is a viable approach for such selective protein capture. Epitope imprinting is a technique to imprint epitope sequence (9-14 mer) of a protein which acts as a signature of specific protein in question (Zahedi et al 2016). Imprinting of epitope sequence obviates the difficulties associated with protein (big molecule with specific folded contours) imprinting under hostile chemical environment. Proteins are inherently dynamic objects, whose conformations have not yet revealed all functions. Epitope imprinting mimics the interaction between antibody and antigen, and it is often used like imprinting of small molecule with surrogate or dummy templates. Using a proper epitope, specially characterized the target protein, is essential for imprinting. It is postulated that the most suitable epitope sites would usually occur in a surface available regions of a protein with flexible structures [14]. Computational approaches were applied for candidate T-cell epitopes prediction from outer membrane proteins (OMP) Por B of N. meningitidis (MC58) (Shah et al 2010). The predicted nonamer epitopes (170GRHNSESYH179 in loop IV) are present on the exposed surface of immunogenic loops of Class 3 OMP allele of N. meningitidis (Shah et al 2010). In our earlier work on proposing epitope imprinted polymer sensors of two

DOI: http://dx.doi.org/10.37398/JSR.2020.640144

computationaly identified epitope sequences for detection of N.meningitidis bactrium, piezoelectric transducers (EQCM) were used for quantifications (Gupta et al 2016, 2018). Here, we are attempting another approach by using an electropolymerizable monomer, 3-thiophene acetic acid and a redox probe is used for quantifications in addition of piezoelectric transducer.

II. Materials and Methods

A. Reagents and materials

3-thiophene acetic acid (99%) was purchased from Sigma-Aldrich, St. Louis, USA. Disodium hydrogen orthophosphate (anhydrous) and sodium dihydrogen orthophosphate (dehydrate) were obtained from Fisher Scientific, Mumbai, India. The computationally derived epitope CGRHNSESYH, interferents epitopes were synthesized and obtained from GenScript, NJ, USA. Globulin and albumin proteins were purchased from M.P. Biomedicals, LLC, France. All chemicals and solvents were of analytical reagent grade, and used without further purification. Human blood plasma samples were collected from Institute of Medical Science (IMS), Banaras Hindu University (BHU) (Varanasi, India) as per approved protocol by the institutional ethical committee of the IMS, BHU after patients' written informed consent.

B. Instruments

1) Electrochemical and Piezoelectrogravimmetric Measurements

EQCM measurements were carried out using model 400B series of CHI 410B. It contains a potentiostat/galvanostat (440B), an external box with oscillator circuitry and the EQCM cell. A gold electrode surface was coated on both faces of a 8MHz AT-cut QCM chip with diameter of the quartz crystal as 13.7 mm and the gold electrode coated on quartz crystal has a diameter of 5.11 mm. Gold coated quartz crystal was used as working electrode, a platinum wire and Ag/AgCl electrode were used as counter and reference electrode respectively.

2) Atomic force microscopy measurements

For Atomic force microscopy (AFM) studies, it was performed by instrument Solver Next model of NT-MDT Company which is used for visualization of evaluation of surface dominant feature. The AFM tip used for imaging was soft silicon nitride, covered with reflective gold coating on the back side and it was performed in air. The scanned area of the sample 5nm x 5nm and scan rate of AFM was 0.5Hz. AFM images were analyzed using image-processing software (Nova PX) to calculate the RMS roughness value.

3) Contact Angle Measurements

Contact angles of water were measured by contact angle goniometer equipped with CCD camera (model HO-IAD-CAM-01) from Holmarc Opto Mechatronics Pvt Ltd., India. This was measured by using the sessile drop method.

4) UV- Vis and Fluorescence Spectroscopy

UV-Visible spectrum was taken by Cary 50 Bio (Varian Instrument Inc. Melbourne, Australia). PerkinElmer LS-55 fluorescence spectrometer was used for recording fluorescence spectra.

C. Modification of EQCM Electrodes

Before modification, the quartz crystal microbalance (QCM) crystal chip was cleaned by piranha solution (1:3, 30% H2O2: concentrated H2SO4) for 1 min and dried with nitogen.QCM electrode was treated with 0.5 mM epitope sequence [in 20 mM PBS, pH 7] for 24 h due to presence of S-containing amino acid cysteine group which was attached in epitope sequence (CGRHNSESYH). A decrease of ~ 415 Hz in resonating frequency of quartz crystal was observed on formation of self assembled monolayer (SAM) of this peptide sequence on gold surface. Schematic presentation of imprinting protocol is shown in Fig 1.

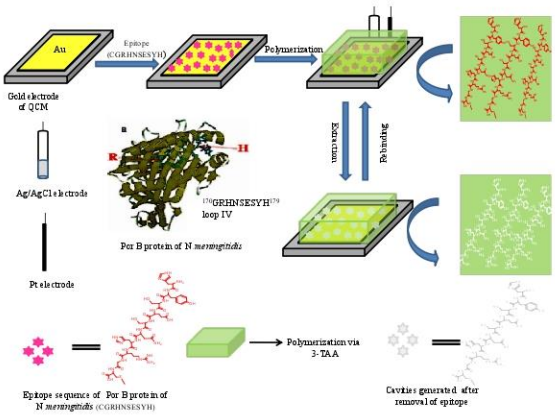

Figure 1: Schematic representation of the epitope-oriented surface imprinting for the preparation of EIP films on a QCM electrode

D. Preparation of epitope imprinted polymer (EIP)

EQCM electrode with SAM of epitope sequence was connected to the instrument and electro polymerization of 3-TAA on the modified EQCM electrode was carried by cyclic voltammetry (CV) in potential range between −0.50 and +1.50 V at a scan rate of 0.10 V/s using Ag/AgCl as reference, Pt wire as counter electrode and PBS as a supporting electrolyte. 3-TAA (8 mmol/L) was dissolved in 8 mL C2H5OH /H2O solution having volume ratio (1:1) in presence of phosphate buffer solution (PBS, pH 7). Non-imprinted polymer (NIP) was also prepared in similar manner without the template (CGRHNSESYH) in polymerization step. Figs 2 (a) and 2 (b) show CV for poly-(3-TAA) film in presence of epitope sequence (EIP) and in absence of template (NIP) at gold electrode respectively.

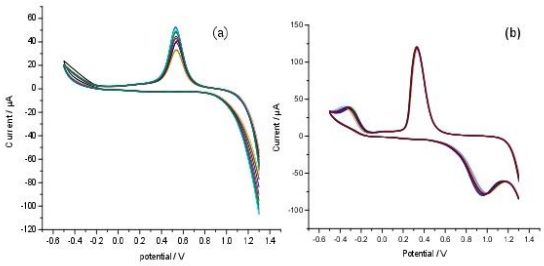

Figure 2: Cyclic voltammograms of the imprinted (a) and non-imprinted polymer (b) films on gold electrode: potential cycling from -0.5 to 1.50 V at a scan rate of 0.10 V/s for 12 cycles with 0.5mM epitope solution, 2.0 mM 3-TAA and PBS as the supporting electrolyte

E. Extraction of Epitope sequence from EIP film

After electropolymerization, EIP film was first rinsed thoroughly with copious amount of water to remove all physisorbed species. Subsequently, electrodes were treated with phosphate buffer solution (PBS) [25 mM, pH 7] for sequestration of peptide sequence resulting in EIP film on gold surface of EQCM electrode. Removal of peptide sequence from the polymeric film was verified by increase in resonating frequency of quartz crystal on which imprinted polymer film-coated gold electrode is mounted till it reaches saturation (Fig 3 (a)). Extraction was further verified by UV-Vis spectra, fluorescence spectra (Figs 3(b) and (c)) and AFM images of imprinted surface (Fig S1).

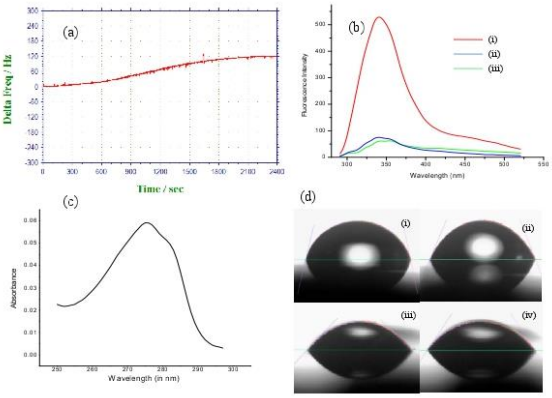

Figure 3: Characterization for extraction: (a) Enhancement in resonating frequency of EIP- modified quartz crystal on repetitive washing with phosphate buffer solution (PBS) till saturation predicting extraction of epitope self-assembled monolayer (SAM), (b) Fluorescence emission spectra of epitope solution (i), extracted solution of epitope (ii) and blood serum of patients suffering from brain fever(iii) respectively in PBS, (c) UV-Visible spectra of extracted solution of epitope concentration in PBS, (d) Contact angles of epitope self-assembled monolayer (SAM) (i), adduct (with template) (ii) and after washing with PBS (iii and iv)

F. Rebinding of Epitope sequence with EIP and NIP film coated EQCM Electrodes

To study the rebinding capacity of epitope sequence, a series of solutions with varying concentration of analyte was prepared and directly added on the gold surface of QCM for electrochemical analysis. All electrochemical runs for each concentration of test analyte were quantified using the differential pulse voltammetry (DPV) analysis of redox probe solution [0.1M K3Fe(CN)6 in the presence of PBS (10mM pH 7)] following the method of standard addition as reported in literature (Tang et al 2014), briefly, an initial peak current (Io) of the DPV was recorded when the imprinted electrode was immersed in the 0.1 M K3Fe(CN)6 solution. The imprinted electrode was then incubated in different concentrations of epitope solutions and washed with water carefully. Afterwards, the imprinted sensor was immersed in the K3Fe(CN)6 solution and the peak DPV current (Ix) was re-recorded. The sensor response was obtained from the change in the reduction current of the K3Fe(CN)6 solution and was calculated from the difference between Io and Ix ($\Delta I = Io-Ix$). To demonstrate the MIP sensor reproducibility, results were averaged for five consecutive measurements.

Rebinding measurements of epitope sequence to epitope imprinted polymer thin film coated EQCM electrode were performed with various concentrations (from 0 to 70 ng mL-1) of epitope which was directly added to the electrochemical cell for analysis. To demonstrate the EIP sensor reproducibility, results were averaged for five consecutive measurements. LOD was calculated as three times the standard deviation from blank measurement (in absence of epitope) divided by slope of calibration plot between analyte (epitope) concentration and change in resonating frequency (Skoog et al 1998). Piezoelectric measurements as well as electrochemical measurements, as mentioned above, were also carried out with NIP-coated QCM electrodes under similar operating conditions.

G. Selectivity evaluation

The affinity of EIP-sensor for template, template structural analogues was evaluated individually by equilibrium binding experiments. The structural analogues were consisting of amino acid residues present in template molecule (CGRHNSESYH), such as GRHNSESYHW, VQKAVGSILVAG, KGLVDDADIC, KPYAKNSVALQAVC and plasma proteins (globulin, albumin).

III. Results and Discussion

A. Synthesis and characterization of EIPs

Fig. 1 shows the sequence of steps involved in grafting of epitope imprinted polymers (MIP) on gold coated EQCM electrode. Epitope sequences CGRHNSESYH were tethered on gold surface of EQCM chip via thiol chemistry of SH present in cysteine amino acid residue. A decrease of ~ 415 Hz in

resonating frequency of quartz crystal was observed on formation of SAM of this peptide sequence on gold surface. This epitope grafted surface of gold coated quartz chip was used to electropolymerized monomer solution (3-TAA). 3-TAA is an advantageous monomer for imprinting as its carboxyl groups are not involved in polymer chain forming reactions and free for interacting with complementary functional groups available on chosen analyte/template (here epitope sequence) (Malitesta et al 2010). Hitherto, 3-TAA has not been utilized for imprinting any epitope/peptide as per our literature survey. Polymeric network was interwoven around SAM sequences tethered on EQCM electrode surface. EQCM monitoring enabled the study of mass loading on electropolymerization and simultaneously assessment of viscoelastic behaviour of film by following resistance change of modified crystal. NIP-coated EQCM electrodes were also prepared similarly without SAM of peptide sequence.

Figs 2(a) and (b) shows the CV recorded during electropolymerization for both MIP and NIP films, oxidation waves can be observed in both voltammogramms respectively. Two peaks are clearly visible in NIP due to oxidation of monomer 3-TAA whereas in MIP only one peak is observed indicating the interaction between epitopes' functional groups with those of 3-TAA. Simultaneous monitoring of piezoelectric behavior of quartz electrode attested the deposition of mass on gold surface of EQCM which formed a rigid polymer layer (Fig S2 (a)). Fig S2 (b) showing resistance change during polymerization, verifies a rigid layer of polymer film as resistance change in quartz crystal is a measure of viscoeleasticity of film adhered to it. Hydrophilic interactions between functional groups of amino acid residues of peptide sequence (-OH,-COOH, CHO,-NH2) and free carboxyl group of poly (3-TAA) are major driving forces for imprinting.

EQCM crystal was repetitively washed with PBS (25 mM) to extract peptide sequence from polymeric matrix in subsequent step until steady state Δf of EQCM electrode was attained (Fig. 3(a)). PBS was chosen as extracting solvent as it has been reported to be efficient in removing thiolated SAMs from gold surface (Flynn et al 2003), and its biocompatibility is expected to maintain the specificity of imprinted sites in residual extracting solution.

Contact angle of water on modified surfaces substantiated the sequence of reactions shown in Fig. 3(d) and Table 1. Contact angle of water on epitope-tethered gold-coated EQCM electrode is ~ 60o showing the hydrophilic nature of peptide sequences attached on gold surface and attests the SAM formation. On electropolymerization, it increased to ~ 77o showing the hydrophobic nature of polymeric matrix interwoven around SAM of peptide sequence. On complete extraction of peptide sequence from polymeric matrix, contact angle reached to ~ 42o showing hydrophilic nature owing to the free carboxyl groups of poly (3-TAA) which were earlier present in conjugation with functional groups of amino acid residues present in peptide sequence.

Table 1: Contact angle of water on epitope-self assembled monolayer (SAM), adduct formation through polymerization, and washing with phosphate buffer solution (PBS, pH 7)

Electrode	Contact angle (o)
Epitope modified	60.35
Adduct modified	76.89
MIP modified	42.27


manuscript-ABC.docx

Fig. S1 shows AFM images of MIP (a) and NIP (b) coated EQCM electrode. Image of MIP shows rough surface with cavities created on imprinting uniformly spread whereas NIP shows a smoother surface as compared to MIP although the polymerization on both electrodes were carried out under similar conditions except using the epitope sequence during polymerization (Table 2). AFM image was profiled for film thickness as well as cavities' thickness (Fig. S1 (c)). It was calculated to be 4-5 nm in MIP film. Hence, a thin homogenous imprinted polymeric sensing layer is fabricated on gold coated quartz crystal.

Table 2: Comparative analysis of atomic force microscopy analysis of epitope imprinted polymer (EIP)-coated and non-imprinted polymer (NIP)-coated quartz crystal microbalance electrode

	Roughnessrms	Roughnessav
EIP	1.295 nm	1.020 nm
NIP	0.912 nm	0.708 nm

Photo physical properties of tyrosine residue were exploited for confirming the imprinting sequence (Figs 3(b) and (c)). Fluorescence spectra shown in Fig. 3 (b) showed a broad and strong emission band around 300–550 nm (excitation wavelength 340 nm), which is typical of tyrosine residue. Hence emission behavior of extracted solution indicated that template molecule was extracted from the imprinted matrix of MIPs. Extracted solution was also examined for UV-Vis absorbance showing absorbance at 274 nm (Fig. 3 (c)). The emission study of template solution also displayed a characteristic excitation

wavelength centered at 340 nm with high intensity in Fig. 3(b) (i) and the extracted solution of template as well as extracted solution from modified electrode after treatment with blood serum of N. meningitidis affected patient has also shown emission in the similar region but with low intensity (Fig. 3 (b) (ii and iii)).

B. Rebinding of epitope sequences on EIP film

To evaluate the recognition ability of MIP modified electrode, epitope sequence solutions of varying concentration were exposed to it. On successive addition of this solution to electrochemical cell, subsequent decrease in resonating frequency is observed due to loading of epitope sequences in the specific cavities created in MIP film coated on EQCM electrode (Fig 4(a)). Inset of Fig 4(a) shows the change in resistance of MIP-coated EQCM electrode. Mass and viscoelastic contributions to the frequency shift can be analyzed from the relation between resistance increase and frequency shift (Lucklum et al 1999). The firm entrapment of peptide molecules in specific cavities created in coated MIP film is evinced by the minimal change in resistance of the coated quartz crystal demonstrating firmness of epitope sequence binding to MIP film although resonating frequency has decreased for ~ 20 Hz due to loading of epitope sequence (CGRHNSESYH).

Fig 4(b) shows frequency shifts of MIP coated EQCM electrode at various concentrations reaching saturation at 50-70 ng.ml-1. K3Fe(CN)6 was used as redox probe for indirect estimation of epitope solution concentration (Fig 4 (c). The peak current of probe gradually decreased with addition of epitope sequences, as the specific cavities entrap epitope molecules, the redox probe could not diffuse to electrode surface, thus diminishing the current. Fig 4 (d) shows the calibration plot for MIP- sensor on rebinding of template, good linear relationship was obtained with R2 = 0.9688.

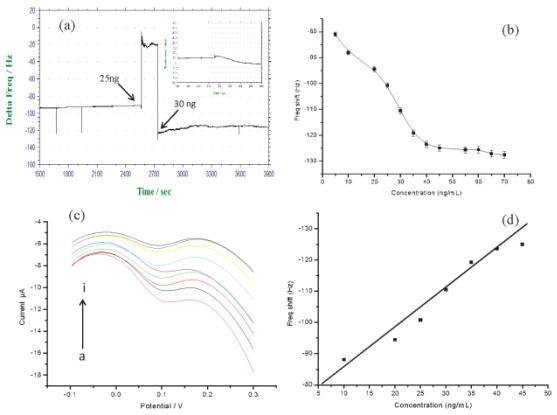

Figure 4: Characterizsations for rebinding: (a) Changes in EIP-coated EQCM frequency in response to different concentration of template [Inset Fig: changes in resistance of EIP-coated EQCM electrode demonstrating viscoelasticity of coated layer], (b) Changes in EIP-coated EQCM frequency in response to varying concentration of epitope, (c) Variation of current of the DPV plots of 0.1 M K3Fe(CN)6, solution having different concentrations of epitope sequence CGRHNSESYH , a) 5, b)10 , c) 15 , d) 20 , e) 25, f) 30, g) 35, h) 40,i) 45 ng. 4-d. Calibration graph of EIP-coated QCM electrode in response to varying concentration of analyte epitope [R2 = 0.9688]

Detection limit for CGRHNSESYH template in aqueous solution by MIP-EQCM sensor is calculated as 9.87 ng.ml-1 (3σ) following standard analytical method (Skoog et al 1998). Linear plot of current difference using the redox probe against concentration of epitope molecule and with blood serum of patients suffering from brain-fever is shown in Fig S3.

C. Binding performance of epitope sequence in EIP and NIP

Fig. 5(a) shows the response of MIP and NIP modified EQCM electrodes towards the peptide sequence. The binding curves for MIP shows a steady decline with concentration as peptide sequences get driven towards their specific cavities but NIP data shows a positive frequency drift, i.e. peptide sequences are free to move around in the solution although similar polymeric matrix is grafted on EQCM electrode in absence of any driving force responsible for binding. But as the concentration rises, they get adsorbed on the non-imprinted polymeric matrix loosely as evident by slight decline in frequency of ~22 Hz. While in the similar concentration range, MIP showed a decline of ~127 Hz and also firm adherence (minimal resistance drift) before reaching saturation. These non-specific bindings (observed in NIP) could be driven by overcrowding of peptide molecules in the vicinity of grafted polymeric matrix (Fig 5 (a)). Imprinting factor (IF) of MIP is found to be 3.83 for the epitope sequence, verifying the selectivity of peptide compared with NIP coated EQCM electrode.

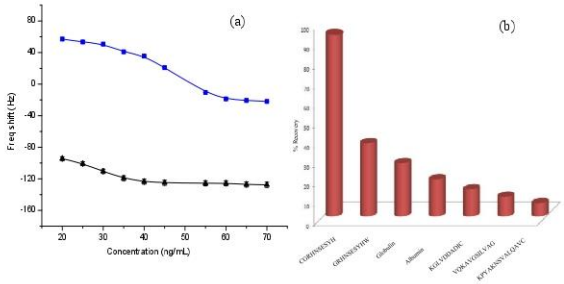

Figure 5: (a) Frequency shift of EIP-coated QCM electrode (▲) and NIP-coated QCM electrode (■) in response to varying concentration of analyte epitope). (b) Changes in EIP-coated QCM frequency in response to various structural analogues [CGRHNSESYH (Cys-Gly-Arg-His-Asn-Ser-Glu-Ser-Tyr-His), GRHNSESYHW (gly-arg-his-asp-ser-glu-ser-tyr-his-trp), globulin, albumin, KGLVDDADIC (lys-gly-leu-val-asp-asp-ala-asp-ile), VQKAVGSILVAG (val-gln-lys-ala-val-gly-ser-ile-leu-val-ala-gly) KPYAKNSVALQAVC (lys-pro-tyr-ala-lys-asn-ser-val-ala-leu-glu-ala-val-cys)]

D. Selectivity evaluation

One of the most important aims of using molecular imprinting

is to reach as high chemo sensing selectivity with respect to analyte analogues as possible. Interaction between plasma proteins (albumin, globulin), peptide sequences either with one amino acid mismatch (GRHNSESYHW (gly-arg-his-asp-ser-glu-ser-tyr-his-trp)), or sequences positioned at exposed surface of immunogenic loops of Class 3 outer membrane protein (OMP) of N. meningitidis (KGLVDDADIC (lys-gly-leu-val-asp-asp-ala-asp-ile)), or of other proteins fbpA and frpB of N. meningitidis (VQKAVGSILVAG (val-gln-lys-ala-val-gly-ser-ile-leu-val-ala-gly), KPYAKNSVALQAVC (lys-pro-tyr-ala-lys-asn-ser-val-ala-leu-glu-ala-val-cys)) and MIP were examined. These peptide sequences comprise of constituent amino acids of template peptide sequence however they are positioned differently from template peptide sequence. The imprinted cavities created in MIP are complementary to that particular template molecule which enables binding of the whole protein molecule via chosen epitope sequence. GRHNSESYHW epitope with only one amino acid mismatch from analyte sequence shows only a little binding followed by plasma proteins, globulin and albumin while other epitope sequences are feebly absorbed. This suggests that a single amino acid mismatch is not endured and binding is grossly affected (Fig. 5(b)). Hence epitope approach of protein imprinting has huge prospects for selective protein sensing. Dismal binding of plasma proteins (globulin, albumin) attests the lack of restrictions from matrix effect. This approach obviates the pre-treatment needed in other biosensing experiments with biological fluids.

Selectivity of MIP was also verified by viscoelasticity of coated film through resistance measurements. Resistance of EQCM electrodes on addition of varying concentration of epitope molecule as well as structural analogues shows that the change was minimal due to firm entrapment of epitope molecule (Figs S4-S10) while on addition of interferrent molecules, change in resistance is large due to loosely bound, feebly adsorbed sequences on MIP film showing high viscoelasticity.

E. Real sample (N. meningitidis infected Blood serum) response

EIP-EQCM sensor thus developed for sensing Por B protein of N.meningitidis was examined with blood serum of patients suffering from meningitis disease. On exposure to blood serum of patients, frequency of EIP-coated EQCM crystal diminishes with varying concentration of blood serum. This decline of frequency saturates on exhausting the number of imprinted cavities on MIP sensor surface (Fig 6(a)). The prepared sensor is able to sense and take up proteins present in N. meningitidis bacterium without any clinical pretreatment of blood serum. Additionally, a redox probe K3[Fe(CN)6] was also tested for indirect estimation of protein uptake in blood serum of patients (Fig. 6(b)). Peak current of probe gradually decreased with addition of blood serum due to entrapment of proteins. As the specific cavities entrap protein molecules, the redox probe could not diffuse to electrode surface, thus diminishing the current (Fig 6(b)).

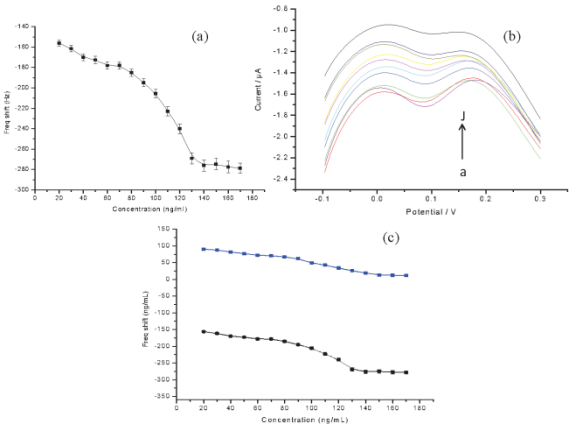

Figure 6: (a) Changes in EIP-coated QCM frequency in response to sequential concentration of serum from patients suffering from brain fever caused by Neisseria meningitidis bacteria, (b) Variation of current of the DPV plots of 0.1 M K3Fe(CN)6, solution having sequential concentrations of epitope sequence CGRHNSESYH , a) 5, b)10 , c) 15 , d) 20 , e) 25, f) 30, g) 35, h) 40,i) 45, j) 50 ng. (c) Changes in EIP-coated QCM frequency in response to sequential concentration of blood serum of patients suffering from brain fever (●) and blood serum of healthy human (■)

F. Prospects for diagnostic application

In the medical diagnostics area, there is always concern about the possibility of false positives and false negatives in any diagnostic test. Here, an attempt is made to diagnose the disease 'brain fever' with this MIP-EQCM sensor thus developed for sensing Por B protein of N. meningitidis. Fig 6(c) shows comparative study of blood serum of patients suffering from brain fever and blood serum from healthy human being was carried out. Resonating frequency increase, in case of healthy human, (as shown by in graph, curve a, Fig 6(c)) whereas under the similar experimental conditions, blood serum of patients suffering from brain fever, MIP film showed large decline in resonating frequency predicting the uptake of proteins present in blood serum of brain fever affected patients demonstrating the preliminary success in achieving the completeness of objective of this experiment i.e. creation of protein sensor through epitope imprinting approach, thus this MIP sensor specifically and selectively diagnoses presence of bacteria proteins in the sample of blood serum affected by N.menigitidis bacteria.

CONCLUSION

The present work was intended to propose a rational approach to protein and peptide imprinting. In the case of a protein when its entire structure is difficult to imprint, short peptides exposed on the surface (epitopes) have been used to prepare a MIP that

later is expected to bind the native protein. Epitope targeted MIP was successfully developed on the gold surface of EQCM electrode with electropolymerization of 3-TAA monomer and demonstrated its application for detection of real samples. High affinity of the epitope-imprinted film towards the template molecule was observed at nanogram range and the LOD value for the epitope molecule was circulated to be 9.87 ng mL-1. These results show advantages of epitope-imprinting such as high sensitivity and high selectivity for the epitope molecule and its native protein present in blood serum of N. meningitidis. Thus the simplicity of the presented method would put forward the facile diagnosis of meningitidis diseases (brain fever) without cumbersome preclinical treatments.

Acknowledgements: Authors acknowledge Institute of Medical Sciences, Banaras Hindu University, Varanasi for providing the blood samples of N.meningitidis bacteria infected patients and financial support by Council of Scientific and Industrial Research (CSIR), New Delhi [No 01(2769)/13/EMR-II]. Authors also acknowledge Department of Science and Technology (DST) New Delhi [SR/S1/IC-25/2011] for instrumental facility (PerkinElmer LS-55 fluorescence spectrometer) provided to Prof D S Pandey, Department of Chemistry, Institute of Science, New Delhi.

REFERENCES

Baethegan LF, Moraes C, Weidlich L, Rios S, Kmetzsh CI, Silva MSN, Rossetti MLR, Zaha A (2003) Direct-test PCR for detection of meningococcal DNA and its serogroup characterization: standardization and adaptation for use in a public health laboratory. J Med Microbiol 52:793–799.

Carrol ED, Thomson APJ, Shears P, Gray SJ, Kaczmarski EB, Hart CA (2003) Performance characteristics of the poly merase chain reaction as s a y to confirm clinical m eningococcal disease .Arch Dis Children 83:271–273.

Deivanayagam N, Ashok TP, Nedunchelian K, Ahamed SS, Mala N (1993) Evaluation of CSF variables as a diagnostic test for bacterial meningitis. J Trop Pediatr 39:284–287.

Dunbar SA, Eason RA, Musher DM, Clarridge JE (1998) Microscopic examination and broth culture of cerebrospinal fluid in diagnosis of meningitis. J Clin Microbiol 36:1617–1620.

Flynn NY, Tran TNT, Cima MJ, Langer R (2003) Long-term stability of self-assembled monolayers in biological media. Langmuir 19:10909-10915.

Gray LD, Fedorko DP (1992) Laboratory diagnosis of bacterial meningitis Clin. Microbiol. Rev. 5:130–145.

Gupta N, R.S. Singh, K. Shah, R. Prasad, M. Singh (2018) Epitope imprinting of iron binding protein of Neisseria meningitides bacteria through multiple monomers imprinting approach J. Mol. Recogn. In Press.doi:10.1002/jmr.2709

Gupta N, Shah K, Singh M (2016) An epitope imprinted piezoelectric diagnostic tool for Neisseria meningitidis detection J. Mol. Recogn., 29: 572-579.

Kilian M, Sorensen I, Frederiksen W (1979) Biochemical characteristics of 130 recent isolates from Haemophilus influenzae meningitis. J Clin Microbiol 9:409–412.

Kotilinen P, Jalava J, Meurman O, Lehtonen OP, Rintala E, Pekka O, La S, Eerola E, Nikkari S (1998) Diagnosis of meningococcal meningitis by broad-range bacterial PCR with cerebrospinal fluid. J Clin Microbiol 36:2205–2209.

Lucklum R., C. Behling, P. Hauptmann (1999) Role of mass accumulation and viscoelastic film properties for the response of acoustic-wave-based chemical sensors Anal. Chem. 71, 2488-2496.

Malitesta C, Guascito MR, Mazzotta E, Picca RA (2010) X-Ray Photoelectron Spectroscopy characterization of electrosynthesized poly (3-thiophene acetic acid) and its application in Molecularly Imprinted Polymers for atrazine . Thin solid films 518:3705–3709.

Neewcombe J, Cartwright K, Palmer WH, Mcfadden J (1996) PCR of peripheral blood for diagnosis of meningococcal disease. J Clin Microbiol 34:1637–1640.

Patel MK, Solankic PR, Kumara A, Khareb S, Gupta S, Malhotrac BD (2010) Electrochemical DNA sensor for Neisseria meningitidis detection. Biosens Bioelectron 25:2586–2591.

Radstrom P, A. Backman, N. Qian, P. Kragsbjerg, C. Pahlson, P. Olcen (1994) Detection of bacterial DNA in cerebrospinal fluid by an assay for simultaneous detection of Neisseria meningitidis, Haemophilus influenzae, and streptococci using a seminested PCR strategy, J. Clin. Microbiol, 32, 2738-2744.

Shah K, Chaubey P, Mishra N (2010) Bioinformatics approach for screening and modeling of putative T cell epitopes from Por B protein of Neisseria meningitides as vaccine constructs. Indian J Biotechnol 9:351-359.

Sippel JE, Hider PA, Controni G, Eisenach KD, Hill HR, Rytel MW, Wasilauskas BL (1984) Use of the directigen latex agglutination test for detection of Haemophilus influenzae, Streptococcus pneumoniae, and Neisseria meningitidis antigens in cerebrospinal fluid from meningitis patients. J Clin Microbiol 20:884–886.

Skoog DA, Holler FT, Nieman TA (1998) Principles of Instrumental Analysis, Harcourt Brace College Publishers 5th ed. Florida 13-14.

Surinder K, Bineeta K, Megha M (2007) Latex particle agglutination test as an adjunct to the diagnosis of bacterial meningitis. Ind J Med Microbiol 25:395–397.

Tan CT, Kuan BB, (1987) Cryptococcus meningitis, clinical—CT scan considerations Neuroradiology 29:43–46.

Tang Q, X. Shi, X. Hou, J. Zhou, Z. Xu (2014) Development of molecularly imprinted electrochemical sensors based on Fe 3 O 4@ MWNT-COOH/CS nanocomposite layers for detecting traces of acephate and trichlorfon. Analyst, 139,

6406-6413.

APPENDIX

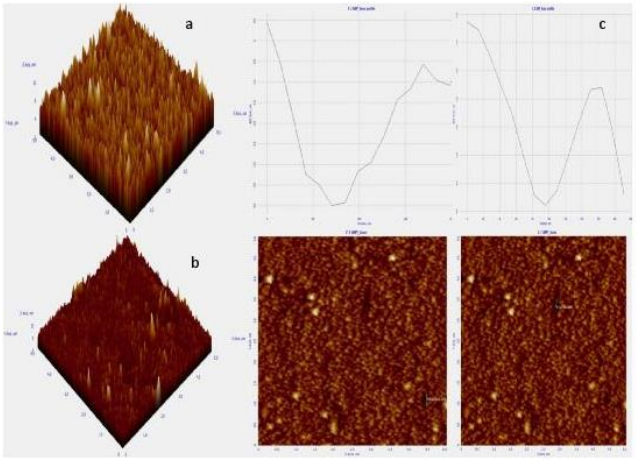

Figure S1: Atomic force microscopy images of (a) molecularly imprinted polymer-coated quartz crystal microbalance electrode and (b) non-imprinted polymer-coated quartz crystal microbalance electrode (c) Profiling of cavities shown in AFM images for estimating thickness of polymer grafted on quartz crystal

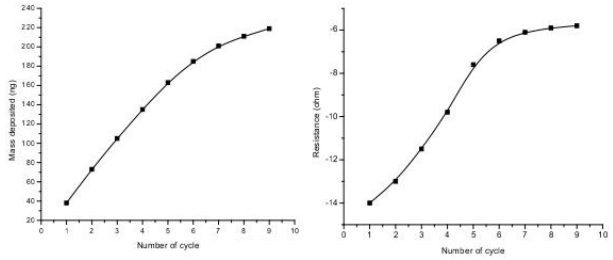

Figure S2: Mass loading and resistance change on electropolymerization of 3-TAA on EQCM electrode

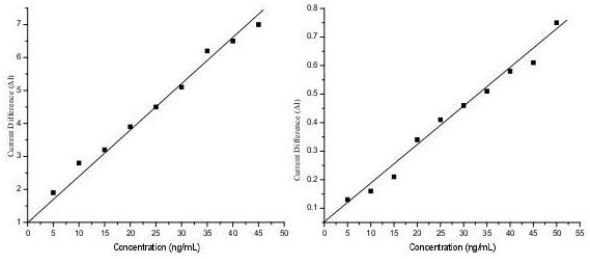

Figure S3: Monitoring of rebinding through electropolymerization with probe (a) at various concentration of epitope molecule (b) at various concentration of blood serum of patient suffering from brain-fever.

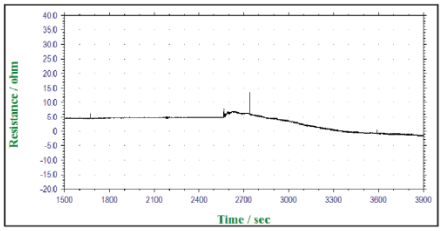

Figure S4: Time-Resitance profile of MIP-coated EQCM electrode in response to epitope molecule

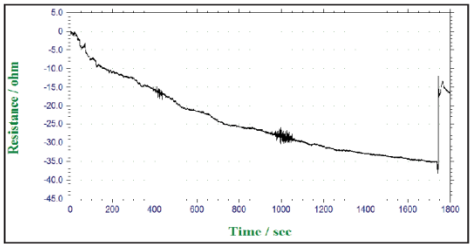

Figure S5: Time-Resitance profile of MIP-coated EQCM electrode in response to structural analogue GRHNSESYHW (gly-arg-his-asp-ser-glu-ser-tyr-his-trp)

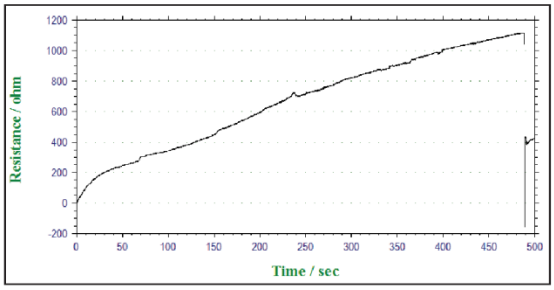

Figure S6: Time-Resitance profile of MIP-coated EQCM electrode in response to structural analogue globulin

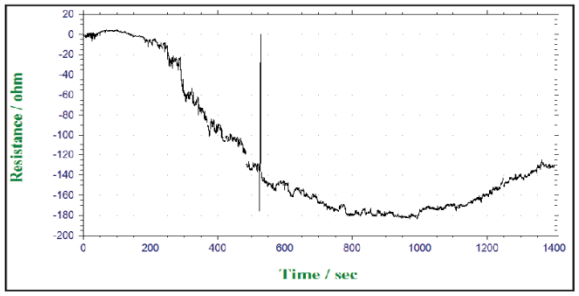

Figure S7: Time-Resitance profile of MIP-coated EQCM electrode in response to structural analogue albumin

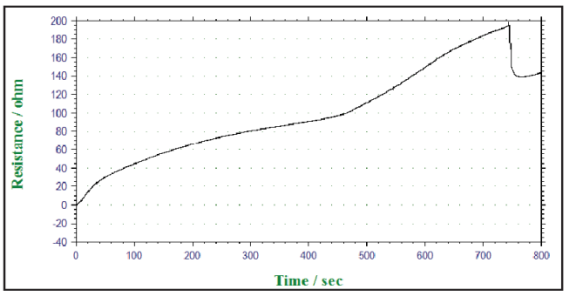

Figure S8: Time-Resitance profile of MIP-coated EQCM electrode in response to structural analogue KGLVDDADIC (lys-gly-leu-val-asp-asp-ala-asp-ile)

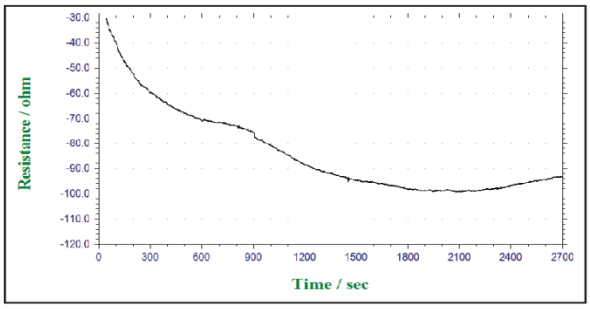

Figure S9: Time-Resitance profile of MIP-coated EQCM electrode in response to structural analogue VQKAVGSILVAG (val-gln-lys-ala-val-gly-ser-ile-leu-val-ala-gly)

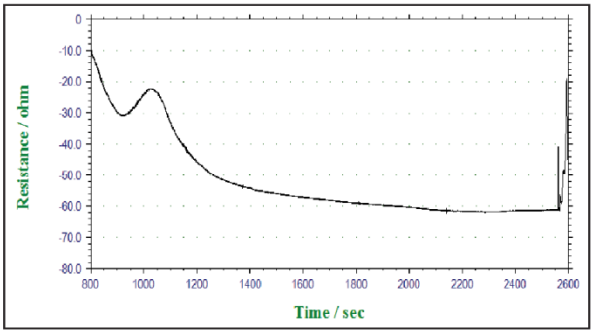

Figure S10: Time-Resitance profile of MIP-coated EQCM electrode in response to structural analogue KPYAKNSVALQAVC (lys-pro-tyr-ala-lys-asn-ser-val-ala-leu-glu-ala-val-cys)

***